nature geoscience

LETTERS

PUBLISHED ONLINE: 26 JULY 2009 | DOI: 10.1038/NGEO587

Constraints on future sea-level rise from past sea-level change

Mark Siddall[1]*†, Thomas F. Stocker[2] and Peter U. Clark[3]

It is difficult to project sea-level rise in response to warming climates by the end of the century, especially because the response of the Greenland and Antarctic ice sheets to warming is not well understood[1]. However, sea-level fluctuations in response to changing climate have been reconstructed for the past 22,000 years from fossil data, a period that covers the transition from the Last Glacial Maximum to the warm Holocene interglacial period. Here we present a simple model of the integrated sea-level response to temperature change that implicitly includes contributions from the thermal expansion and the reduction of continental ice. Our model explains much of the centennial-scale variability observed over the past 22,000 years, and estimates 4–24 cm of sea-level rise during the twentieth century, in agreement with the Fourth Assessment Report of the Intergovernmental Panel on Climate Change[1] (IPCC). In response to the minimum (1.1 °C) and maximum (6.4 °C) warming projected for AD 2100 by the IPCC models, our model predicts 7 and 82 cm of sea-level rise by the end of the twenty-first century, respectively. The range of sea-level rise is slightly larger than the estimates from the IPCC models of 18–76 cm, but is sufficiently similar to increase confidence in the projections.

Understanding the sea-level response to global warming is required for mitigating and adapting to future climate change. Strategies to address this problem include not only enhanced observations but also improvements to deterministic models of the response of glaciers and ice sheets to global warming[2], modelling studies of previous interglacials[3], model estimates of changes to ice-sheet surface mass balance due to climate change[4], modelled changes to ocean heat and freshwater budgets[5] and constraining a simple empirical model of the acceleration in sea-level rise due to global warming[6,7]. Given that each of these approaches has its limitations, it is important to consider alternative approaches to determine the reproducibility of the projections of sea-level rise over the next century.

We develop a new approach to estimate sea-level rise over the coming century using reconstructions of sea-level rise since the Last Glacial Maximum (LGM), which occurred ~21,000 years ago. These data constrain several periods of large and unambiguous sea-level rise on centennial timescales, which represent integrated contributions from ice sheets, glaciers and thermal expansion—all of the likely contributors to sea-level rise in the twenty-first century. In particular, using these data allows us to evaluate the nonlinear response of the integrated sea-level response to large temperature changes.

We first define a function to describe the theoretical state that sea level would attain with respect to temperature in the absence of any perturbation. We will call the sea level defined by this function the equilibrium sea level. Note that we are concerned with defining this function during the last termination and acknowledge that it may well have a different form during the onset of glaciation

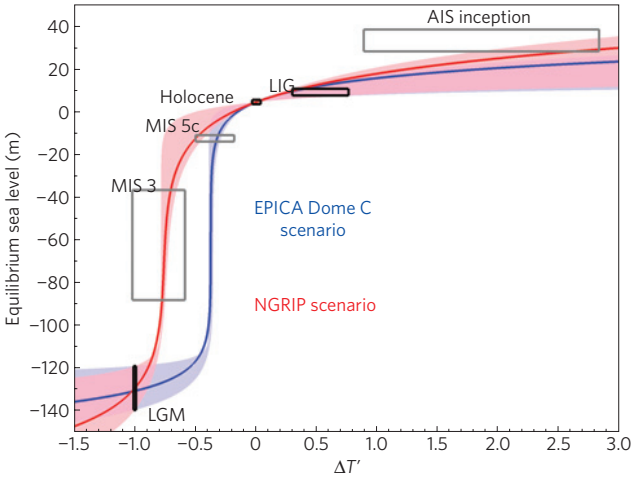

Figure 1 | The best fit equilibrium sea-level curve for the simulations considered as a function of $\Delta T'$. $\Delta T' = (T - T_{\mathrm{Holocene}})/\Delta T_{\mathrm{LGM}}$. The rectangles are observational estimates during periods that may have been close to equilibrium sea level, except MIS 3. MIS 5c taken from ref. 24 and inception of the Antarctic ice sheet (AIS) taken from ref. 25. As sea level is highly sensitive to temperature change at intermediate temperatures, it is difficult to define a period when sea level reached equilibrium at such temperatures. During MIS 3, temperature varied on millennial timescales over a 30 kyr period (60–30 kyr ago; ref. 26). Given that the timescale of ice-sheet response is several thousand years, sea level should have varied around the equilibrium position during this period[11]. As a constraint on sea-level sensitivity during this period we therefore take the range of observed sea level (−40 to −90 m; refs 11, 27). Temperatures either represent values presented in Supplementary Table S1 (LIG, LGM) or the mean and standard deviation of the variability in NGRIP (ref. 17) and EPICA Dome C (ref. 18) scenarios combined over the respective periods (Holocene: 2–0 kyr BP, MIS 3: 60–30 kyr BP and MIS 5c: 105–100 kyr BP) (see summary in Supplementary Table S1). The best fit curve and error estimates are generated from the complete, time-dependent model and are not a function of the fit to the grey rectangles—MIS 3, MIS 5c and AIS values (grey) are not used to constrain the model but are simply shown here for comparison. The curve is constrained to pass though Holocene, LGM and LIG values (black). Equilibrium sea level is given relative to late Holocene values (0 m).

[1]Lamont Doherty Earth Observatory of Columbia University, 61 Route 9W, PO Box 1000, Palisades, New York 10964-8000, USA, [2]Climate and Environmental Physics, Physics Institute, University of Bern, Bern, CH 3012, Switzerland, [3]Department of Geosciences, 104 Wilkinson Hall, Oregon State University, Corvallis, Oregon 97331-5506, USA. *Present address: Department of Earth Sciences, University of Bristol, Wills Memorial Building, Queen's Road, Bristol BS8 1RJ, UK. †e-mail: mark.siddall@bristol.ac.uk.

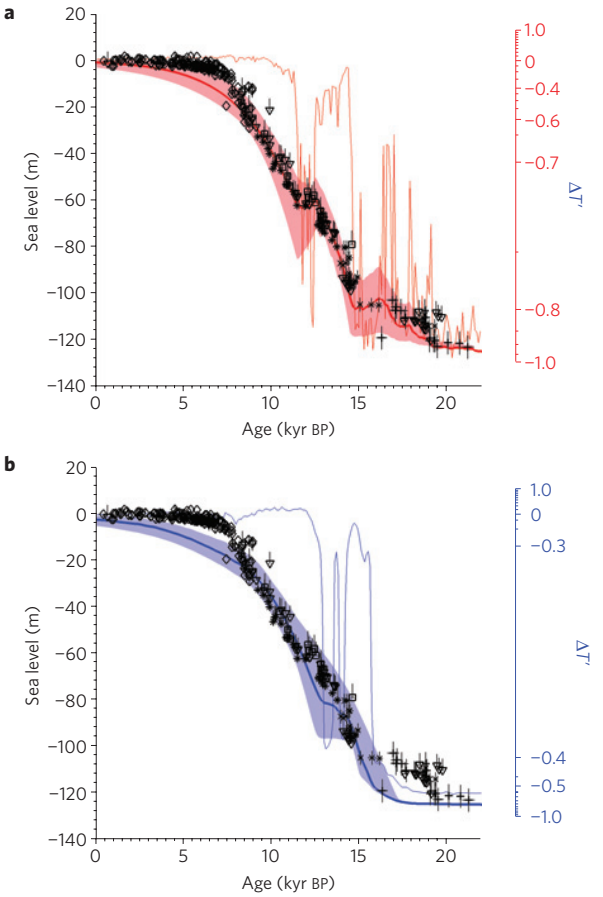

Figure 2 | Model simulation of the termination. a,**b**, Optimum simulations are shown as thick lines for the NGRIP scenario (red) and the EPICA Dome C scenario (blue) . Uncertainty intervals are shown as the lighter-coloured patches. Also shown are the equilibrium sea levels (thin lines) derived from the ice-core records. The equilibrium sea levels correspond to the ice-core temperature records at a given $\Delta T'$, which is shown on the nonlinear scales to the right of the plots. The sea-level proxy data are marked as black symbols (see Supplementary Fig. S1 for key and references). Sea level is given relative to late Holocene values.

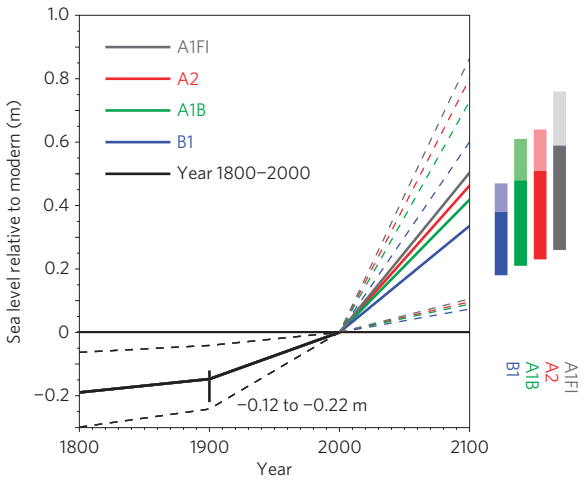

Figure 3 | Model projections of sea-level rise for the twenty-first century. The best estimate projections are shown as solid lines; the range is shown by the dashed lines. The range of projected sea-level rise takes into account the temperature range from IPCC for individual emissions scenarios, uncertainty in ΔT_{LGM}, which is taken to be 3.3–5.1 °C with a best estimate of 4.2 °C, and uncertainty in the warming estimate from the past century (0.56–0.92 °C, with a best estimate of 0.74 °C; ref. 1). For comparison, IPCC estimates (mean from 2090 to 2100) for individual emissions scenarios are given by the coloured vertical bars on the right. The lighter part represents the extended IPCC (ref. 1) estimate allowing for the extra contribution of 0.09–0.17 m sea-level rise due to accelerated ice-sheet dynamics under a warmer climate. The vertical black line represents sea level in 1900, allowing for a rise in sea level of between 0.12 and 0.22 m over the 1900s. Values are shown in Table 1.

due to ice sheet/climate feedbacks. In defining this function, we need to account for several physical effects that have been shown to be robust features of ice-sheet growth and decay during the last glacial period in both proxy reconstructions and numerical models of ice sheets (see further discussion in Supplementary Information). As a result of these well-documented processes, ice-sheet size and sea level have a tendency to remain close to glacial maximum or minimum, with relatively rapid retreats from maxima, and into and out of minima, triggered by crossing thresholds in the nonlinear system. This hysteresis behaviour has been described in simple models for Northern Hemisphere ice sheets[8] and for East Antarctica[9]. Quaternary sea-level data over the past 500,000 years support this concept in suggesting two quasi-equilibrium states (interglacial and glacial)[10–12] that are separated by rapid transitions[13]. Therefore, we represent the equilibrium sea level (S_e) as a function of the inverse hyperbolic sin ($\sinh^{-1}$) with respect to temperature:

$$S_e = A\sinh^{-1}\left(\frac{\Delta T' + c}{b}\right) + d \qquad (1)$$

where $\Delta T'$ is defined as the non-dimensional change in temperature with respect to mean late Holocene temperatures (2 kyr BP to present). Temperature is non-dimensionalized with respect to ΔT_{LGM}, the difference in temperature between the late Holocene and the LGM, so that $\Delta T' = (T - T_{Holocene})/\Delta T_{LGM}$. All of the variables used in this letter are summarized and defined in Supplementary Table S1. Note that S_e is constrained to pass through values for the Last Interglacial[14,15] (LIG; see the Methods section).

Figure 1 shows the best-fit sea-level sensitivity curves that are used in this letter. We note that the $\sinh^{-1}$ function derived here (equation (1)) passes through several independent constraints on the sea-level sensitivity curve. The model results indicate a much reduced sensitivity for warmer temperatures compared with LGM temperatures, implying that the negative feedbacks in operation at the glacial maximum are relatively weak compared with the feedbacks at glacial minimum. Further discussion of the sensitivity of our method for different functions for S_e is given in Supplementary Information.

Next we define a response time, τ (in units of kyr), that defines the rate at which the modelled sea level (S_m) rises in response to an increase in equilibrium sea level in a similar fashion to an earlier study [6], so that at time t:

$$\frac{dS_m}{dt} = r \cdot \frac{1}{\tau} \cdot [S_e(\Delta T'(t)) - S_m(t)] \times \begin{cases} r = 1, & \text{if} \quad S_e(\Delta T'(t)) > S_m(t) \\ 0 < r < 1, & \text{if} \quad S_e(\Delta T'(t)) < S_m(t) \end{cases} \qquad (2)$$

where τ is a typical response time of sea-level rise following a shift in temperature. We have introduced a factor r (varied between 0 and 1) that permits us to take into account the fact that sea-level rise due to ice-sheet decay is faster than sea-level

Table 1 | Model projections of sea-level rise for various IPCC scenarios for the twenty-first century.

	Temperature change (°C)		Published sea-level rise (m)	Model projections of sea-level rise (m)	
	Best estimate*	Range	Range	Best estimate*	Range
Pre industrial				0.04	0.02–0.06
Fleming *et al.*[28]	—	—	0.04–0.06†	—	—
Church *et al.*[19]	—	—	0.02–0.06	—	—
Domingues *et al.*[29]	—	—	0.02	—	—
1900–2000					
IPCC[1]	0.74	0.56–0.92	0.12–0.22	0.15	0.04–0.24
2090–2100 (mean)					
IPCC[1] scenario A1FI	4.0	2.4–6.4	0.26–0.59 (0.76§)	0.48	0.10–0.82‡
IPCC[1] scenario A2	3.4	2.0–5.4	0.23–0.51 (0.64§)	0.44	0.09–0.76‡
IPCC[1] scenario A1B	2.8	1.7–4.4	0.21–0.48 (0.61§)	0.40	0.08–0.69‡
IPCC[1] scenario B1	1.8	1.1–2.9	0.18–0.38 (0.47§)	0.32	0.07–0.57‡

*Refers to estimates forced by the model optimized values and the mean or 'best estimate' from the IPCC scenarios.

†Note that Fleming *et al.*[28] suggest a possible reduced rate of sea-level rise over the past 2 kyr compared with the period between 7 and 2 kyr ago.

‡The range of projected sea-level rise takes into account the temperature range for individual emissions scenarios[1], uncertainty in ΔT_{LGM}, which is taken to be 3.3–5.1 °C with a mean value of 4.2 °C, and uncertainty in the warming estimate from the past century (0.56–0.92 °C, with a best estimate of 0.74 °C (ref. 1)).

§Increased upper limit on range, allowing for increased rise due to uncertainty in the contribution from accelerated ice-sheet dynamics.

fall due to ice-sheet growth[16]. In equation (2), the sea-level rise is fastest following a period of large warming, whereas rapid cooling would cause a longer response time τ/r. As we are considering a period dominated by sea-level rise, the model is not sensitive to the precise value of r. We include r for completeness and to consider the possibility of any brief sea-level lowering during the Younger Dryas cold period or the Antarctic cold reversal (see Supplementary Fig. S1, see sensitivity tests in Supplementary Information). Note that the use of a single timescale to represent the integrated contributions of ocean thermal expansion, glacier retreat and changes in ice sheets is an important simplification that limits the useful application of the model to centennial and longer-term responses (see Supplementary Section S6.2).

As r varies between periods of sea-level increase and decrease, it is not possible to solve equation (2) in closed form. Instead sea level is given by integrating (2) over time steps $\Delta t = 0.1$ kyr so that:

$$S_m(t+\Delta t) = S_m(t) + r \cdot \frac{\Delta t}{\tau} \cdot \left[S_e(\Delta T'(t)) - S_m(t)\right] \qquad (3)$$

where r takes the appropriate value depending on the sign of $S_m(t) - S_e(\Delta T'(t))$. The precise value of time step Δt that is used has no impact on our results.

Equations (1) and (3) require that we define the history of the temperature variability that forced changes in sea level over the last deglaciation. During the last deglaciation, millennial variability affected temperatures differently in the Northern and Southern hemispheres[17,18]. We therefore consider two temperature proxy alternatives to represent the temperature forcing of sea level during the deglaciation: the oxygen isotope ($\delta^{18}O$) record of the North Greenland Ice Core Project[17] (NGRIP) (representative of the Northern Hemisphere) and the deuterium (δD) record of the European Project for Ice Coring in Antarctica (EPICA) Dome C (ref. 18) (representative of the Southern Hemisphere) (see Supplementary Fig. S1). We provide an evaluation of each of these scenarios in Supplementary Information. We will call the scenarios: 'the NGRIP scenario' and 'the EPICA Dome C scenario'.

We require some means to evaluate and tune the model output over the past 22 kyr. We define the proportion of the variance explained by the model (R^2, see Supplementary Equation S1) by comparing the model estimate with the estimate from sea-level proxies (S_{proxy}). Observational constraints (S_{proxy}) of sea-level rise are based on indicators of past sea level recorded at sites distant from the principal ice sheets ('far-field' sites). Sea-level indicators such as fossil corals or other depth-dependent coastal deposits reflect isostatic effects associated with the ice–water surface mass redistribution as well as variations in global (eustatic) sea level. A full discussion of these data and a note on the effect of isostatic rebound are given in Supplementary Information.

Figure 2 shows the model simulations of the past 22 kyr for both the NGRIP and EPICA Dome C forcing scenarios. These simulations allow for uncertainty in the data and input variables (see the Methods section). Significantly, the NGRIP scenario captures a number of details in the structure of the sea-level record during the different phases of the deglaciation (post-LGM, Bølling–Allerød warming, Younger Dryas cooling, post-Younger Dryas warming and so on), whereas the EPICA Dome C scenario does not (in particular note the deviations during the post-LGM period, the Antarctic cold reversal and the transition to the Holocene). Despite these discrepancies, the R^2 for the optimal solution is only slightly higher for the NGRIP scenario than for the EPICA Dome C scenario (0.99 compared with 0.97). Therefore, we distinguish the success of the NGRIP compared with the EPICA Dome C simulations on the basis of its ability to capture the structure of the sea-level rise. In addition, the best-fit equilibrium sea-level curve (Fig. 1) for the NGRIP scenario passes through the independent estimates from Marine Isotope Stage 3 (MIS 3) and the initiation of the Antarctic ice sheet, whereas the curve for the EPICA Dome C scenario does not. On the basis of these findings, we reject the EPICA Dome C scenario and focus on the NGRIP scenario for the remainder of the letter.

We note that the deglaciation comprises several periods with large changes in sea level on centennial timescales (in particular at the time of the Bølling–Allerød warming and the warming following the Younger Dryas). As these periods of rapid change represent a substantial proportion of the total sea-level rise during the deglaciation, we are confident that the model is capable of resolving sea-level change on centennial timescales. We test this assertion in Supplementary Information where we force

the model with the annual mean temperature record for the twentieth century and compare it with the annual mean sea-level record (see Supplementary Fig. S5). The offsets between the model and data over this period are an order of magnitude smaller than the sea-level rise over the twentieth century and are linked to decadal fluctuations in sea level rather than the centennial trend. We conclude that the model can resolve sea-level rise on centennial timescales (but not decadal), and it is reasonable to approximate the contributions to sea-level rise from multiple sources (that is, glaciers, ice sheets and thermal expansion) with one, integrated model. As the anthropogenic temperature perturbation began around 1900 and possibly earlier[7], by 2100 this perturbation will have lasted at least two centuries. It is important for this application that the model is tuned to multi-centennial records.

The NGRIP scenario shows continuing sea-level rise of 0.02–0.06 m per century before the industrial period (Figs 2a and 3, Table 1), in close agreement with other estimates derived using independent methods (see Supplementary Table S1). Given that the model successfully simulates the sea-level variability over the past 22 kyr (Fig. 2a) and the twentieth century (see Supplementary Fig. S5), we next use the model to make projections of the model response to future warming.

Over the twenty-first century, projected sea-level rise reaches a maximum of 0.82 m in response to warming from the upper estimate of the A1FI emissions scenario (6.4 °C) and a minimum of 0.07 m rise for the lower warming estimate for the B1 emissions scenario (1.1 °C, Fig. 3 and Table 1). These extremes in our model projections compare to IPCC estimates of 0.59 m for the upper limit of the A1FI scenario and 0.18 m for the lower limit of the B1 scenario[1]. Our estimates converge more closely with IPCC estimates when including the extra 0.09–0.17 m rise that the IPCC's fourth assessment report estimated was the potential contribution over the next century from accelerated ice-sheet dynamics[1]. A substantial portion of the uncertainty intervals calculated here and those of the IPCC simulations intersect and our results generally increase the confidence that one may have in the IPCC results. As the time constant of the sea-level response is 2,900 years, our model indicates that the impact of twentieth-century warming on sea level will continue many centuries into the future and therefore constitutes an important component of irreversible climate change in the future. Our results indicate the importance of cumulative anthropogenic warming over several centuries on sea-level rise as recognized in IPCC reports[19].

Methods

We define $\Delta T'$ with reference to the NGRIP (ref. 17) and EPICA Dome C (ref. 18) ice-core proxy temperature (T) reconstructions. The value of ΔT_{LGM} for each of the ice-core proxy records is taken as the mean value between 25 and 20 kyr BP so that $\Delta T' = (T - T_{\mathrm{Holocene}})/\Delta T_{\mathrm{LGM}}$.

In equation (1), the variable b controls the slope of S_e with respect to $\Delta T'$ and c controls the midpoint of the transition in S_e with respect to $\Delta T'$ (see sensitivity study in Supplementary Information). We vary c and b and then scale A so that S_e gives the correct magnitude of change at the LGM (Fig. 1). For the purpose of this study, we assume an LGM sea level of between −120 and −140 m (refs 20, 21). We then adjust d so that S_e passes through the Holocene value (0 m). The variable b controls the difference in S_e between the late Holocene period and the LIG. We randomly vary b so that S_e passes through the sea-level estimates of 3–6 m above modern for the LIG (ref. 14, 15) (Fig. 1). The variable c is controlled by the period of rapid sea-level change associated with the termination. The value of c is left unconstrained and is given by the model optimization.

To constrain b, we need to define $\Delta T'$ for the LIG. We derive the temperature difference between the Holocene period and the LIG (~125,000 years ago), ΔT_{LIG} ($\Delta T_{\mathrm{LIG}} = T_{\mathrm{LIG}} - T_{\mathrm{Holocene}}$), from ice-core temperature constraints (3–5 °C) (ref. 22), assuming a polar amplification factor of two[23] to give the global mean estimate of 1.5–2.5 °C. To obtain $\Delta T'_{\mathrm{LIG}}$, we need to define the global mean ΔT_{LGM}. On the basis of a compilation of model estimates, we take ΔT_{LGM} to be between 3.3 and 5.1 °C, with a preferred estimate of 4.2 °C (ref. 1). Note that by defining $\Delta T'$ and a given polar amplification factor, the warmth of the LIG compared with the Holocene is relative so that the same value represents relative polar warming or the global mean warming. An obvious concern with using LIG values is that insolation forcing was not the same during the LIG compared with the Holocene. Rohling *et al.*[12] recently showed a close relationship between sea level and temperature over the past 525 kyr on multi-millennial (that is, quasi-equilibrium) timescales, indicating a close coupling of temperature and sea level regardless of large changes in insolation. This justifies our assumption that increased temperature can be considered the primary driver of higher sea level during the LIG.

Using the proxy sea-level data, equations (1) and (3) are optimized to give the maximum value for R^2 using the lsqcurvefit function in the Matlab Optimisation toolbox. The model is initiated at a sea level of −130 m. The model is not sensitive to the sea level at which it is initiated. To avoid sampling bias associated with the increased data density during the Holocene we carry out 10,000 simulations, each time fitting the model to a different, randomly sampled and evenly distributed subset of half of the proxy observations. To account for the uncertainty in the proxy observations, we randomly vary the data in the stated uncertainty range for each sample, assuming that this uncertainty is normally distributed. In this way we are able to estimate each of the variables by taking the mean of each variable weighted to the R^2 value for all of the simulations. We are also able to estimate the uncertainty associated with each of the variables.

For the projections, we force the model with a warming of 0.74 °C over the past century[1] and further warming over the next century from the IPCC emissions scenarios[1] (Fig. 3, Table 1). We allow for the range of uncertainty in warming over the past century of between 0.56 and 0.92 °C and for the uncertainty in the projected warming over the coming century for individual emissions scenarios[1] by carrying out multiple simulations representing the maximum, minimum and preferred warming estimates over the past century and the coming century. In each case the uncertainty in the model variables is included to generate a maximum and minimum estimate of sea-level rise for the next century. We remind the reader that by defining $\Delta T'$ and a given polar amplification factor, any future warming is relative, so that the same $\Delta T'$ is representative of polar warming or the global mean warming.

Received 15 May 2008; accepted 29 June 2009; published online 26 July 2009

References

1. IPCC. in *Climate Change 2007: The Physical Science Basis* (eds Solomon, S. *et al.*) (Cambridge Univ. Press, 2007).
2. Alley, R. B., Clark, P. U., Huybrechts, P. & Joughin, I. Ice-sheet and sea-level changes. *Science* **310**, 456–460 (2005).
3. Otto-Bliesner, B. L. *et al.* Simulating Arctic climate warmth and icefield retreat in the last interglaciation. *Science* **311**, 1751–1753 (2006).
4. Gregory, J. M. & Huybrechts, P. Ice-sheet contributions to future sea-level change. *Phil. Trans. R. Soc. A* **364**, 1709–1731 (2006).
5. Gregory, J. M., Lowe, J. A. & Tett, S. B. T. Simulated global-mean sea-level changes over the last half-millennium. *J. Clim.* **19**, 4576–4591 (2006).
6. Rahmstorf, S. A semi-empirical approach to projecting future sea-level rise. *Science* **315**, 368–370 (2007).
7. Grinsted, A., Moore, J. C. & Jevrejeva, S. Reconstructing sea level from paleo and projected temperatures 200–2100 AD. *Clim. Dyn.* doi: 10.1007/s00382-008-0507-2 (2009).
8. North, G. R. The small ice cap instability in diffusive climate models. *J. Atmos. Sci.* **41**, 3390–3395 (1984).
9. Pollard, D. & DeConto, R. M. Hysteresis in Cenozoic Antarctic ice sheet variations. *Glob. Planet. Change* **45**, 9–21 (2005).
10. Waelbroeck, C. *et al.* Sea-level and deep water temperature changes derived from benthic foraminifera isotopic records. *Quat. Sci. Res.* **21**, 295–305 (2002).
11. Siddall, M. *et al.* Sea-level fluctuations during the last glacial cycle. *Nature* **423**, 853–858 (2003).
12. Rohling, E. J. *et al.* Antarctic temperature and global sea level closely coupled over the last five glacial cycles. *Nature Geosci.* **2**, 500–504 (2009).
13. Cutler, K. B. *et al.* Rapid sea-level fall and deep-ocean temperature change since the last interglacial period. *Earth Planet. Sci. Lett.* **206**, 253–271 (2003).
14. Stirling, C. H., Esat, T. M., Lambeck, K. & McCulloch, M. T. Timing and duration of the last interglacial: Evidence for a restricted interval of widespread coral reef growth. *Earth Planet. Sci. Lett.* **160**, 745–762 (1998).
15. Muhs, D. R. Evidence for the timing and duration of the last interglacial period from high-precision uranium-series ages of corals on tectonically stable coastlines. *Quat. Res.* **58**, 36–40 (2002).
16. Weertman, J. Rate of growth or shrinkage of nonequilibrium ice sheets. *J. Glaciol.* **6**, 145–158 (1964).
17. NGRIP members, High-resolution record of Northern Hemisphere climate extending into the last interglacial period. *Nature* **431**, 147–151 (2004).
18. EPICA Members, Eight glacial cycles from an Antarctic ice core. *Nature* **429**, 623–628 (2004).
19. Church, J. A. *et al.* in *Climate Change 2001: The Scientific Basis* (eds Houghton, J. T. *et al.*) 639–694 (Cambridge Univ. Press, 2001).

20. Peltier, W. R. & Fairbanks, R. G. Global glacial ice volume and Last Glacial Maximum duration from an extended Barbados sea level record. *Quat. Sci. Rev.* **25**, 3322–3337 (2006).
21. Yokoyama, Y., Lambeck, K., De Deckker, P., Johnston, P. & Fifield, L. K. Timing of the Last Glacial Maximum from observed sea-level minima. *Nature* **406**, 713–716 (2000).
22. Masson-Delmotte, V. *et al.* Past and future polar amplification of climate change: Climate model intercomparisons and ice-core constraints. *Clim. Dyn.* **26**, 513–529 (2006).
23. Hansen, J. *et al.* Climate change and trace gases. *Phil. Trans. R. Soc. A* **365**, 1925–1954 (2007).
24. Schellmann, G. & Radtke, U. A revised morpho and chronostratigraphy of the late and middle Pleistocene coral reef terraces on Southern Barbados (West Indies). *Earth Sci. Rev.* **64**, 157–187 (2004).
25. Lear, C. H. in *Perspectives on Climate Change: Marrying the Signal from Computer Models and Biological Proxies* (eds Haywood, W. M. *et al.*) 313–322 (The Micropalaeontological Society, Special Publications, The Geological Society, 2007).
26. Dansgaard, W. *et al.* in *Climate Processes and Climate Sensitivity* Vol. 29 (eds Hansen, J. E. & Takahashi, T.) 288–298 (Geophys. Monogr. Ser., AGU, 1984).
27. Siddall, M., Rohling, E. J., Thompson, W. G. & Waelbroeck, C. MIS 3 Sea-level fluctuations: Data synthesis and new outlook. *Rev. Geophys.* **46**, RG4003 (2008).
28. Fleming, K. *et al.* Refining the eustatic sea-level curve since the Last Glacial Maximum using far- and intermediate-field sites. *Earth Planet. Sci. Lett.* **163**, 327–342 (1998).
29. Domingues, C. M. *et al.* Improved estimates of upper-ocean warming and multi-decadal sea-level rise. *Nature* **453**, 1090–1093 (2008).

Acknowledgements

M.S. acknowledges support from Lamont Doherty Earth Observatory and the University of Bristol (LDEO and RCUK fellowships). Conversations with J. Shepherd and D. Pollard have been very useful in bringing this work together and it could not have been completed without their suggestions. Support from the Swiss National Science Foundation and the University of Bern (T.F.S.) and the US National Science Foundation (P.U.C.) is acknowledged.

Author contributions

Initial concept: M.S.; development, refinement, writing: M.S., P.U.C., T.F.S.

Additional information

Supplementary information accompanies this paper on www.nature.com/naturegeoscience. Reprints and permissions information is available online at http://npg.nature.com/reprintsandpermissions. Correspondence and requests for materials should be addressed to M.S.